

Effects of surface states on electrical characteristics of InN and $\text{In}_{1-x}\text{Ga}_x\text{N}$

J. W. L. Yim,^{1,2} R. E. Jones,^{1,2} K. M. Yu,² J. W. Ager III,² W. Walukiewicz,²
William J. Schaff,³ and J. Wu^{1,2,*}

¹*Department of Materials Science and Engineering, University of California, Berkeley, California 94720, USA*

²*Materials Sciences Division, Lawrence Berkeley National Laboratory, Berkeley, California 94720, USA*

³*Department of Electrical and Computer Engineering, Cornell University, Ithaca, New York 14853, USA*

(Received 22 May 2007; published 30 July 2007)

Surface states are known to pin the Fermi level in InN and $\text{In}_{1-x}\text{Ga}_x\text{N}$, strongly affecting charge distribution and transport on the surface and at interfaces. By solving Poisson's equation over a range of bias voltages for an electrolyte-based capacitance-voltage measurement configuration, we have calculated the band bending and space charge distribution in this system and developed an electronic model generally applicable to both *p*- and *n*-type group-III-nitride thin films. Both conduction band nonparabolicity and band renormalization effects due to the high surface electron concentration were included. The calculated space charge distributions, using the majority dopant concentration as a fitting parameter, are in excellent agreement with experimental data. The model quantitatively describes increasingly strong *n*-type electrical characteristics on the surface due to electron accumulation in *p*-type $\text{In}_{1-x}\text{Ga}_x\text{N}$ for decreasing values of *x*. This also provides a general understanding of the effect of mobile carriers on capacitance-voltage measurements.

DOI: 10.1103/PhysRevB.76.041303

PACS number(s): 73.20.At, 73.40.Mr, 73.61.Ey

The widely tunable band gaps of the group-III-nitride alloy system present a promising opportunity for optoelectronic and photovoltaic applications.^{1,2} However, progress has been hampered by difficulty in producing *p*-type materials, particularly on the lower band gap end of the $\text{In}_{1-x}\text{Ga}_x\text{N}$ alloy with In-rich compositions. Recent findings using electrolyte-based capacitance voltage measurements provide evidence that it is possible to dope InN *p*-type.^{3,4} However, while a recent calculation confirms bulk *p*-type conductivity across the composition range of $\text{In}_{1-x}\text{Ga}_x\text{N}$,⁵ a method for quantitative evaluation of the active acceptor concentration is still absent due to the complications arising from the presence of donorlike surface states.

It has been recognized that surface states which pin the Fermi level (E_F) tend to fall near a universal energy level, known as the Fermi stabilization energy (E_{FS}).^{3,6} E_{FS} lies 4.9 eV below the vacuum level, coinciding with the so-called branch point energy,⁷ and falls into the band gap for most semiconductors. However, in InN and In-rich $\text{In}_{1-x}\text{Ga}_x\text{N}$ and $\text{In}_{1-x}\text{Al}_x\text{N}$, it is located deep in the conduction band, about 0.8 eV above the conduction band edge (E_C) or 1.5 eV above the valence band edge (E_V) of InN,⁸ due to their exceptionally large electron affinity. This energy configuration causes strong electron accumulation near the surface,^{3,5,8,9} hiding the *p*-type activity in the acceptor-doped bulk. Electrical properties, measured by Hall effect, are determined by electrical transport in the surface layer rather than in the bulk of the sample. Further complications from the conduction band nonparabolicity and band renormalization also arise at such high electron concentrations near the surface.¹⁰

In view of the lack of a complete modeling of this effect in InN and $\text{In}_{1-x}\text{Ga}_x\text{N}$, we calculated the band bending and charge distributions along the depth in both *n*- and *p*-type $\text{In}_{1-x}\text{Ga}_x\text{N}$ as a function of composition, bulk doping, and external bias using Poisson's equation. The calculation took into account the nonparabolicity of the conduction band within the Kane *k*·*p* model and the renormalization effects

due to electron-electron and electron-ion interactions, both of which become significant at high electron concentrations such as in the surface layer.¹⁰ This model was used to quantify active dopants in InN films whose charge concentration profiles were measured using electrolyte-based capacitance voltage (ECV) profiling. Previous work using ECV (Refs. 3 and 4) and the hot probe test¹¹ has provided evidence of *p*-type activity in Mg-doped InN grown by molecular beam epitaxy. Our model quantitatively describes *n*-type electrical behavior at the surface due to electron accumulation in both donor and acceptor doped InN, in agreement with ECV measurements of these films. This model was also applied to the alloy system $\text{In}_{1-x}\text{Ga}_x\text{N}$, providing a method to analyze the doping and space charge profile even in the presence of strong surface accumulation or inversion caused by dense surface states.

The electron potential in InN as a function of depth dictates the band bending and is related to the charge distribution by the one-dimensional Poisson equation,

$$\frac{d^2V(z)}{dz^2} = \frac{e}{\epsilon_0\epsilon_r} \{N_{ad} - n[V(z)] + p[V(z)]\}, \quad (1)$$

where N_{ad} is the charge due to the majority ionized dopant, which equals $-N_a$ if acceptors and N_d if donors. The free electron distribution $n(V)$ is given by the Fermi distribution in conjunction with the density of states of the conduction band,

$$n(V) = \int_{-\infty}^{\infty} \frac{\rho_c(E - V)}{1 + \exp[(E - E_F)/k_B T]} dE, \quad (2)$$

where $\rho_c(E)$ is the density of states calculated from the nonparabolic conduction band dispersion obtained in Kane's *k*·*p* model.¹⁰ A similar expression was used for $p(V)$, assuming a parabolic valence band with effective hole mass of $1.65m_0$.¹² In our simulation, we assume zero current flow, such that E_F is flat throughout the entire film, lining up with E_F at the

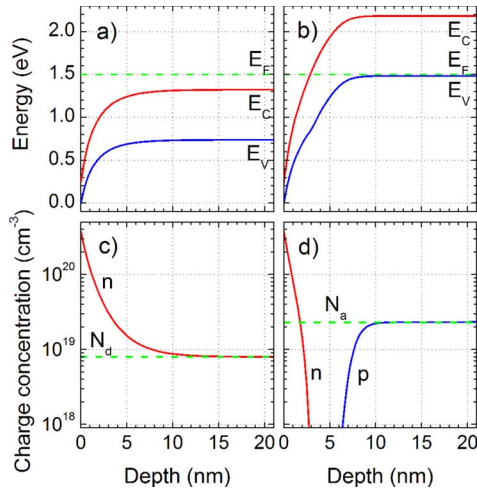


FIG. 1. (Color online) Calculated band diagram and associated carrier concentrations near the surface at zero applied bias for n -type InN doped with $N_d=8 \times 10^{18} \text{ cm}^{-3}$ in (a) and (c), respectively, and for p -type InN doped with $N_a=2.3 \times 10^{19} \text{ cm}^{-3}$ in (b) and (d). For the n -type case, the free hole concentration ($\sim 10^8 \text{ cm}^{-3}$) is negligible, hence it is not pictured.

surface [Fig. 1(a)], which is equal to E_{FS} (1.5 eV above E_V) at zero bias. The conduction band edge E_C at the surface, which sets the boundary condition $V(z)$ at $z=0$, lies at $E_g - \Delta(n)$ above E_V , where $E_g=0.7 \text{ eV}$ and $\Delta(n)$ represents the downward shift of E_C caused by the conduction band renormalization effect from electron-electron and electron-ion scattering.¹⁰ The renormalization effect becomes significant at high electron concentrations such as in the surface accumulation layer discussed here, resulting in a band-gap narrowing of $>0.15 \text{ eV}$ per decade of increase in n when $n > \sim 10^{19} \text{ cm}^{-3}$. On the surface, $\Delta(n)$ was determined by the value of n at $z=0$, which is obtained from solving Eq. (2) self-consistently with $V=V(0)$. The doping level, N_d or N_a , sets the boundary conditions at large depth such that as $z \rightarrow \infty$, $dV(z)/dz \rightarrow 0$ and $V(z)$ is equal to the bulk E_C given by charge neutrality, $n[V(\infty)]=N_d$ or $p[V(\infty)]=N_a$.

Figure 1 illustrates the surface band bending at zero bias for n -type doping of $N_d=8.0 \times 10^{18} \text{ cm}^{-3}$ (a) and for p -type of $N_a=2.3 \times 10^{19} \text{ cm}^{-3}$ (b). In both cases, the conduction and valence bands are bent far below E_F , giving rise to strong electron accumulation on the surface to a depth of $\sim 10 \text{ nm}$. The electron and hole concentrations are shown in Figs. 1(c) and 1(d) for the n - and p -doped films, respectively. For the n -doped film, n decreases from $3.5 \times 10^{20} \text{ cm}^{-3}$ on the surface to N_d in the bulk. In the p -doped film, n drops from $3.5 \times 10^{20} \text{ cm}^{-3}$ on the surface to a negligible minority level in the bulk. This surface inversion layer is followed by a depletion region before eventually reverting to bulk p -type behavior. Hence surface pinning creates a native n^+/p junction at a depth of $\sim 5 \text{ nm}$ in p -doped InN film. This natural shallow junction could be measured in carefully designed experiments and may be exploited for device applications. This demonstrates that surface electron accumulation must be included in interpretations of surface-sensitive spectroscopic and electrical measurements of InN. A similar surface elec-

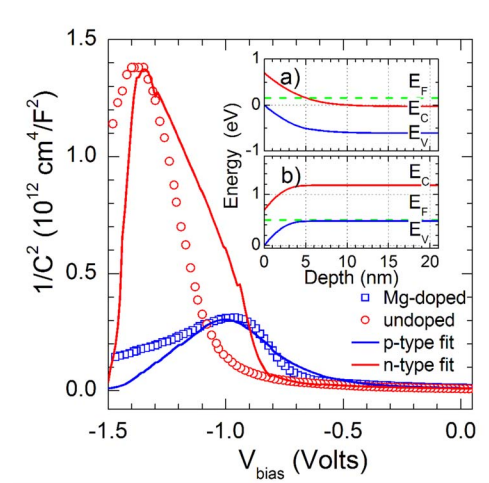


FIG. 2. (Color online) $1/C^2$ as a function of applied bias determined by ECV measurements for unintentionally doped and Mg-doped InN along with two calculated curves for $N_d=8 \times 10^{18} \text{ cm}^{-3}$ and $N_a=2.3 \times 10^{19} \text{ cm}^{-3}$. The inset shows the band bending configuration calculated for the unintentionally doped (a) and Mg-doped (b) films at their respective $V_{\text{bias}}^{\text{peak}}$.

tron accumulation effect was observed in other materials with large electron affinities, such as InAs,¹³ which also has its surface E_F pinned above its E_C . Significant band-gap narrowing due to the band renormalization effect is also evident in this electron accumulation layer. The direct band gap is reduced from the intrinsic $E_g=0.7 \text{ eV}$ to $\sim 0.25 \text{ eV}$ at $z=0$.

Electrical characterizations often use the Hall effect, which measures the free carrier concentration averaged over the depth weighted by mobility. For nonuniform distributions such as these, capacitance-voltage (CV) profiling yields more information as it probes the net charge concentration as a function of depth. However, due to the surface E_F pinned above E_C , the required Schottky contacts for conventional CV profiling have not been achieved. Instead, an electrolyte has been used to form a rectifying contact.^{3,4,13} A bias voltage (V_{bias}) applied to the electrolyte with respect to the grounded sample bulk shifts the surface Fermi level to $E_F=E_{FS}+V_{\text{bias}}$. Thus a negative V_{bias} causes the surface energy bands to move upward relative to E_{FS} , making the surface bands bend less than in Fig. 1(a). At sufficiently large negative V_{bias} , a flat band, followed by surface depletion, and eventually inversion band configuration can be realized for both n - and p -doped films, provided that the electrolyte or film junction does not break down at these voltages.

The total space charge (Q) in the system was calculated over a wide range of V_{bias} by integrating $N_{\text{ad}}-n(z)+p(z)$ over z . The capacitance was computed from $C(V_{\text{bias}})=dQ(V_{\text{bias}})/dV_{\text{bias}}$. The capacitances of an unintentionally n -type-doped and an Mg-doped InN film were measured using the ECV method as a function of bias voltage. Both experimental and calculated data are shown in a Mott-Schottky representation ($1/C^2$ vs V_{bias}) in Fig. 2. A sample-independent voltage offset, known as the rest potential, to account for the difference between E_{FS} and the chemical potential of the electrolyte,¹⁴ was added to the ECV data when

comparing with the calculated curves. A peak occurs for $1/C^2$ with different height and at different $V_{\text{bias}}^{\text{peak}}$ for these two samples.

In conventional C - V experiments in the *depletion* regime on samples with no surface Fermi level pinning, the slope on the Mott-Schottky plot is inversely proportional to the ionized *net-dopant* concentration. For our choice of bias voltage polarity, a negative (positive) slope would indicate a donor (acceptor) doping in the sample. However, in the case of space charge accumulation or inversion which is common for narrow-gap semiconductors at high bias, this simple net-dopant interpretation is no longer valid because mobile carriers are present in significant quantity and contribute to the capacitance reading as well. Surface Fermi level pinning further complicates the picture. Our model accounts for all these effects and agrees well with the ECV data previously used as evidence for p -type activity in Mg-doped InN.³ In fitting to both the peak height and position, the only parameter that was adjusted is the doping level N_a or N_d (aside from the constant rest potential¹⁵). Assuming a majority doping level of $N_d=8.0 \times 10^{18} \text{ cm}^{-3}$, we achieve a good fit to the unintentionally doped InN sample, whose n -type character is most likely due to intrinsic defects from growth, often on the order of mid- 10^{17} to mid- 10^{19} cm^{-3} .¹⁰ In comparison, the Mg-doped InN fit well with $N_a=2.3 \times 10^{19} \text{ cm}^{-3}$, signifying p -type activity below the surface layer in this film. By experimentation, we found that including both the band nonparabolicity and band renormalization effects achieves the best fit with the experimental ECV data.

In both n - and p -type films, C is large (thus $1/C^2$ is small) at small V_{bias} , due to the total space charge (Q) being dominated by electrons accumulated on the surface. This amount is determined by the E_F pinned well above the conduction band E_C and is enhanced by the conduction band nonparabolicity and band renormalization effects. Consequently, Q is very sensitive to the shift of E_F by V_{bias} , which translates to a large $C=dQ/dV_{\text{bias}}$. At a certain $V_{\text{bias}}=V_{\text{bias}}^{\text{peak}}$, however, when the surface E_F is displaced into the band gap, Q becomes desensitized to the change in V_{bias} , because E_F is too far from both E_C and E_V to populate or depopulate the conduction or valence bands. For this V_{bias} , the system has the smallest C and thus has a peak in $1/C^2$. The band configuration at $V_{\text{bias}}^{\text{peak}}$ is depicted in the inset of Fig. 2 for the two films under investigation. As V_{bias} becomes more negative, the surface E_F approaches E_V to induce free holes, such that Q resumes its high sensitivity to V_{bias} . Hence both n - and p -doped InN films show a peak in their Mott-Schottky plots. Therefore a mere change of slope sign in the Mott-Schottky plot is *not* evidence for the presence of surface inversion; rather, as will be shown below, the peak position and height can be used to evaluate the doping type and the bulk doping level, respectively.

As can be seen from the inset of Fig. 2, the position of E_F at $V_{\text{bias}}^{\text{peak}}$ relative to the surface E_V and E_C is not the same for n - and p -doped films. It is closer to E_V (E_C) on the surface for n - (p)-doped InN, resulting in a more negative $V_{\text{bias}}^{\text{peak}}$ for n -doped films than for p -doped ones. The surface E_F position where Q is the least sensitive to changes in V_{bias} is not at the midgap; instead, it is pushed away from the doped band

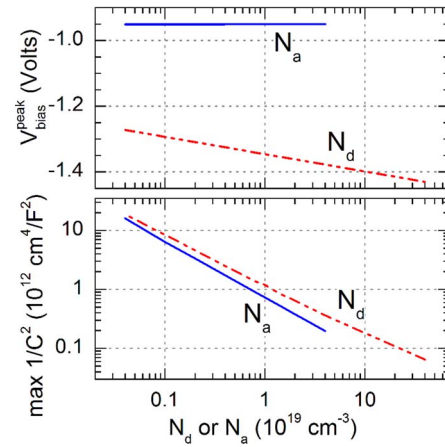


FIG. 3. (Color online) Calculated peak value of $1/C^2$ (lower) and $V_{\text{bias}}^{\text{peak}}$ (upper) as a function of doping level for n - and p -doped InN. Note the logarithmic scales.

since Q changes rapidly at the onset of depletion. This effect breaks the symmetry of the surface E_F in the band gap, and quantitatively identifies the type and level of doping in the bulk from the position and height of the $1/C^2$ peak. In Fig. 3 we show $V_{\text{bias}}^{\text{peak}}$ and the peak height calculated as a function of doping level for both n - and p -doped InN. It can be seen that $V_{\text{bias}}^{\text{peak}}$ is largely independent of N_a for p -type doping, and is more negative and scales approximately logarithmically with N_d within the range of interest for n -type doping. This different behavior arises from the much larger density of states in the valence band than in the conduction band in InN. The peak height scales almost linearly with $1/N_a$ or $1/N_d$ as seen from the log-log plot. When the film is doped with higher N_a or N_d , Q can be changed more rapidly by depleting these dopants even at $V_{\text{bias}}^{\text{peak}}$, which makes it more sensitive to changes in V_{bias} (hence a lower peak height). As ECV is

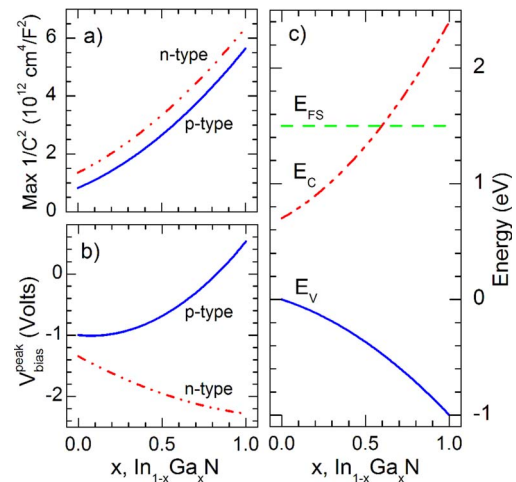


FIG. 4. (Color online) Calculated peak value of $1/C^2$ (a) and $V_{\text{bias}}^{\text{peak}}$ (b) as a function of Ga fraction for n -type and p -type $\text{In}_{1-x}\text{Ga}_x\text{N}$ with a majority dopant level of $8 \times 10^{18} \text{ cm}^{-3}$. (c) Conduction and valence band alignment of $\text{In}_{1-x}\text{Ga}_x\text{N}$ relative to the valence band edge of InN. The Fermi stabilization energy is shown as a reference level.

essentially the only technique for measuring the doping level in the presence of surface accumulation in narrow-gap semiconductors such as InN and InAs, our model provides a general guideline and calibration for analyzing doping levels for narrow-gap semiconductors. The conventional net-dopant interpretation, which relates the sign of slope on the Mott-Schottky plot to the type of doping and the magnitude of the slope to $1/N_a$ or $1/N_d$, is valid only in the regime where the surface is in depletion, i.e., between -1.0 and -1.5 V in Fig. 2.

This model can also be extended to other group-III-nitride systems with similar band structures. We investigated the band bending for the extensively studied $\text{In}_{1-x}\text{Ga}_x\text{N}$ alloys by expressing their E_C and E_V on the absolute energy scale¹⁶ [Fig. 4(c)] and using linear extrapolations between InN and GaN (Ref. 17) for their dielectric constant, carrier effective mass, and other band parameters.¹⁸ Using a doping level N_d or N_a of $8.0 \times 10^{18} \text{ cm}^{-3}$ as an example, we found significant surface electron accumulation, higher than the doping level,

for $x < \sim 0.7$ at zero bias. The $1/C^2$ peak height and position are shown in Figs. 4(a) and 4(b) as a function of x . As expected, the peak in $1/C^2$ for n -type alloys, indicating the turnover from depletion to inversion, occurs at very large negative biases, so they will always exhibit n -type character unless strongly biased without breakdown. For p -type alloys at zero bias, p -type character is evident on the surface only for relatively large Ga fractions. Displacing E_F to near E_V (E_C) on the surface for n (p)-doped alloys maximizes $1/C^2$, such that the shift of $V_{\text{bias}}^{\text{peak}}$ toward negative (positive) directions with increasing x reflects the increasing (decreasing) distance of E_V (E_C) from E_{FS} as illustrated in Fig. 4(c).

This work was supported by the National Science Foundation under Grant No. EEC-0425914. This work is also supported by the Director, Office of Science, Office of Basic Energy Sciences, Division of Materials Sciences and Engineering, of the U.S. Department of Energy under Contract No. DE-AC02-05CH11231.

*wuj@berkeley.edu

¹J. Wu, W. Walukiewicz, K. M. Yu, W. Shan, J. W. Ager III, E. E. Haller, H. Lu, W. J. Schaff, W. K. Metzger, and S. Kurtz, *J. Appl. Phys.* **94**, 6477 (2003).

²V. Y. Davydov *et al.*, *Phys. Status Solidi B* **234**, 787 (2002).

³R. E. Jones, K. M. Yu, S. X. Li, W. Walukiewicz, J. W. Ager III, E. E. Haller, H. Lu, and W. J. Schaff, *Phys. Rev. Lett.* **96**, 125505 (2006).

⁴P. A. Anderson, C. H. Swartz, D. Carder, R. J. Reeves, S. M. Durbin, S. Chandril, and T. H. Myers, *Appl. Phys. Lett.* **89**, 184104 (2006).

⁵P. D. C. King, T. D. Veal, P. H. Jefferson, C. F. McConville, H. Lu, and W. J. Schaff, *Phys. Rev. B* **75**, 115312 (2007).

⁶W. Walukiewicz, *Physica B* **302-303**, 123 (2001).

⁷J. Tersoff, *Phys. Rev. B* **32**, 6968 (1985).

⁸I. Mahboob, T. D. Veal, L. F. J. Piper, C. F. McConville, H. Lu, W. J. Schaff, J. Furthmuller, and F. Bechstedt, *Phys. Rev. B* **69**, 201307(R) (2004).

⁹I. Mahboob, T. D. Veal, C. F. McConville, H. Lu, and W. J. Schaff, *Phys. Rev. Lett.* **92**, 036804 (2004).

¹⁰J. Wu, W. Walukiewicz, W. Shan, K. M. Yu, J. W. Ager III, E. E. Haller, H. Lu, and W. J. Schaff, *Phys. Rev. B* **66**, 201403(R) (2002).

¹¹N. Miller, R. E. Jones, J. W. Ager III, K. M. Yu, E. E. Haller, and W. Walukiewicz (unpublished).

¹²Y. C. Yeo, T. C. Chong, and M. F. Li, *J. Appl. Phys.* **83**, 1429 (1998).

¹³V. Gopal, E. H. Chen, E. P. Kvam, and J. M. Woodall, *J. Electron. Mater.* **29**, 1333 (2000).

¹⁴P. Blood, *Semicond. Sci. Technol.* **1**, 7 (1986).

¹⁵In the ECV experiments we used 0.2–1.0 M NaOH in ethylenediaminetetraacetic acid as the electrolyte; the rest potential used was 0.675 V to align the ECV data with modeled curves.

¹⁶J. Wu, W. Walukiewicz, K. M. Yu, J. W. Ager III, S. X. Li, E. E. Haller, H. Lu, and W. J. Schaff, *Solid State Commun.* **127**, 411 (2003).

¹⁷M. E. Levinshstein, S. L. Rumyantsev, and M. Shur, *Properties of Advanced Semiconductor Materials: GaN, AlN, InN, BN, SiC, SiGe* (Wiley, New York, 2001).

¹⁸I. Vurgaftman and J. R. Meyer, *J. Appl. Phys.* **94**, 3675 (2003).